



Regional Hurst Exponent Reflects Impulsivity-Related Alterations in Fronto-Hippocampal Pathways Within the Waiting Impulsivity Network

Susanne Neufang^{1,2*} and Atae Akhrif^{2,3}

¹ Department of Psychiatry and Psychotherapy, Medical Faculty Heinrich-Heine University, Düsseldorf, Germany,

² Comparative Psychology, Institute of Experimental Psychology, Heinrich-Heine University, Düsseldorf, Germany, ³ Center of Mental Health, Department of Child and Adolescent Psychiatry, University of Würzburg, Würzburg, Germany

OPEN ACCESS

Edited by:

Olga Sosnovtseva,
University of Copenhagen, Denmark

Reviewed by:

Chengyu Huo,
Changshu Institute of Technology,
China
Andras Eke,
Semmelweis University, Hungary

*Correspondence:

Susanne Neufang
neufang@hhu.de

Specialty section:

This article was submitted to
Fractal and Network Physiology,
a section of the journal
Frontiers in Physiology

Received: 14 March 2020

Accepted: 22 June 2020

Published: 10 July 2020

Citation:

Neufang S and Akhrif A (2020)
Regional Hurst Exponent Reflects
Impulsivity-Related Alterations
in Fronto-Hippocampal Pathways
Within the Waiting Impulsivity
Network. *Front. Physiol.* 11:827.
doi: 10.3389/fphys.2020.00827

In general, the Hurst exponent, H , is used as a measure of long-term memory of time series. In previous neuroimaging studies, H has been introduced as one important parameter to define resting-state networks, reflecting upon global scale-free properties emerging from a network. H has been examined in the waiting impulsivity (WI) network in an earlier study. We found that alterations of H in the anterior cingulate cortex (H^{ACC}) and the nucleus accumbens (H^{NAcc}) were lower in high impulsive (highIMP) compared to low impulsive (lowIMP) participants. Following up on those findings, we addressed the relation between altered fractality in H^{ACC} and H^{NAcc} and brain activation and neural network connectivity. To do so, brain activation maps were calculated, and network connectivity was determined using the Dynamic Causal Modeling (DCM) approach. Finally, $1-H$ scores were determined to quantify the alterations of H . This way, the focus of the analyses was placed on the potential effects of alterations of H on neural network activation and connectivity. Correlation analyses between the alterations of H^{ACC}/H^{NAcc} and activation maps and DCM estimates were performed. We found that the alterations of H predominantly correlated with fronto-hippocampal pathways and correlations were significant only in highIMP subjects. For example, alterations of H^{ACC} was associated with a decrease in neural activation in the right HC in combination with increased ACC-hippocampal connectivity. Alteration in H^{NAcc} , in return, was related to an increase in bilateral prefrontal activation in combination with increased fronto-hippocampal connectivity. The findings, that the WI network was related to H alteration in highIMP subjects indicated that impulse control was not reduced *per se* but lacked consistency. Additionally, H has been used to describe long-term memory processes before, e.g., in capital markets, energy future prices, and human memory. Thus, current findings supported the relation of H toward memory processing even when further prominent cognitive functions were involved.

Keywords: Hurst exponent, fMRI, neural network connectivity, impulsivity, fronto-hippocampal pathways

INTRODUCTION

The Hurst exponent H is used as a measure of long-term memory of time series (Eke et al., 2000). In previous neuroimaging studies, H has been introduced as one important parameter to define resting-state networks (Taylor et al., 2012), reflecting upon global scale-free dynamics emerging from a network (Mukli et al., 2018). As real-world time series in general and neuroimaging data in particular, often do not fulfill the criteria of self-similarity or other fractal properties, fractal methods have been further extended. For example, long-range dependence and self-similarity have been shown to be strongly interrelated (e.g., Pipiras and Taqqu, 2017), thus, the application of fractal approaches on time series showing long-range dependence has been encouraged (Abry et al., 2013). Furthermore, the irregularity of a signal plays a crucial role, and that “this irregularity contains meaningful information” (Abry et al., 2013, pp. 19–20).

Among other cognitive functions, H has been linked to human memory processing mathematically (Namazi, 2018) as well as in numerous neuroscientific studies. For example, Wink et al. (2006) showed in a resting-state fMRI study, that bilaterally in the hippocampus (HC) H increased with age (Wink et al., 2006) in healthy subjects. In addition, H seemed to be a sensitive parameter to detect changes in HC processing in patients with and without memory disturbances, e.g., reduced hippocampal H in patients with mild cognitive impairment (Long et al., 2018), autism spectrum disorder (Dona et al., 2017a), and mild traumatic brain injury (Dona et al., 2017b). Furthermore, (multi)fractal analysis of fMRI has been used to “disentangle functional components from artifactual ones, in a robust and significant manner.” (Ciuciu et al., 2012) and to differentiate between healthy neural network from impaired ones at the example of the waiting impulsivity (WI) network in an earlier publication (Akhrif et al., 2018). WI is defined as the ability to inhibit a response in order to earn a reward (Voon et al., 2014). The WI network includes the ventromedial and dorsolateral prefrontal cortex (dlPFC) representing motor or response inhibition (Mechelmans et al., 2017), the reward perception-related nucleus accumbens (NAcc), the anterior cingulate cortex (ACC) for the cognitive evaluation of the reward and HC and amygdala (AMY) responsible for reward-based learning (Dalley et al., 2011). In an earlier study, we found that, H in the ACC and NAcc was reduced in high impulsive (highIMP) compared to low impulsive (lowIMP) participants (Akhrif et al., 2018). Very recent studies showed, that functional connectivity between the ACC and NAcc in the WI network varied in function of monetary reward (high reward, strong connectivity, and vice versa, Mechelmans et al., 2017) and that especially H in the ACC was associated with impulsivity (Gentili et al., 2020).

Following up on the earlier findings, we addressed the relation between the impulsivity-related H reductions in the NAcc and the ACC and brain activation and neural network connectivity of the entire WI network in this study. To do so, brain activation maps were generated, and network connectivity was determined using the Dynamic Causal Modeling (DCM) approach. DCM quantifies the influence region A has on a second region B; thus, it reveals the causal structure of a network. In a final step,

H scores as described earlier were transferred into deviations from $1H$. H valued close to 1 in the fMRI signal has been associated with highly complex and well attuned dynamics in neural networks (Lipsitz and Goldberger, 1992; Goldberger et al., 2002). In the earlier publication we showed that H values for highIMP subjects (i.e., impaired network functioning) were significantly lower than in lowIMP subjects. Therefore, the question to tackle in the current analyses was, how the deviation from 1 was related to brain activation and effective network connectivity. To address the relation between altered fractality and the network, correlation analyses were performed using H deviations and brain activation maps as well as DCM estimates. This way, the focus of the analyses was placed on the potential effects of alterations of H on neural network activation and connectivity.

MATERIALS AND METHODS

Subjects

In this pilot study, we examined 103 male students, aged between 19 and 28 years (24.0 ± 2.6 years). Volunteers were recruited at the University of Wuerzburg, Germany, and screened for impulsivity using the Wender-Reimherr-Interview and Attention-Deficit/Hyperactivity Disorder checklist (subscales “impulsivity” and “hyperactivity and impulse control”; Rösler et al., 2008; for details see Neufang et al., 2016). The study was conducted in accordance with the Declaration of Helsinki in its latest version from 2008 and was approved by the ethics committee of the Faculty of Medicine, University of Wuerzburg. Their written informed consent was obtained from all volunteers.

Experimental Paradigm

As cognitive task, the human version of the five choice serial reaction time task (5-CSRTT; animal version 5-CSRTT: Bari et al., 2008; human version, 4-CSRTT: Voon et al., 2014) was used. A trial started with a short presentation of 4 boxes, followed by a target in terms of a green dot, located in one of the four boxes. Correct and quick responses were reward by two amounts of money (10 Cent, 1 Euro). Premature responses were defined as reactions before target onset (for a representative trial see **Supplementary Figure S1**). The task consisted of one block outside the scanner (2.5 min) and five blocks within the MR scanner (14 min) with each block consisting of 20 trials. Total task duration was 16.5 min (for further detail Neufang et al., 2016).

Behavioral testing started with a first baseline block outside the scanner, conducted to determine the individual mean reaction time window ($rt, M_{rt} \pm 2 SD$). The individual rt windows were used for reward definition in all consecutive blocks, which were performed in the MR scanner: one Euro if the subject responded correct and faster than the individual rt window, 10 cent if the subjects' responses were within the same. Incorrect answers were neither rewarded nor punished.

Data Acquisition

MRI scanning was performed using a 3 Tesla TIM Trio Scanner (Siemens, Erlangen, Germany). Functional MRI included a

T2*-weighted gradient echo-planar imaging sequence with the following parameters: repetition time (TR) = 2000 ms, echo time (TE) = 30 ms, 36 slices of 3 mm thickness, field of view (FoV) = 192 mm, flip angle = 90, and number of volumes = 425.

Data Processing and Time Series Extraction

fMRI-data processing was performed using the Statistical Parametric Mapping Software Package (SPM12, Wellcome Department of Imaging Neuroscience, London, United Kingdom, Wellcome Trust Center for Neuroimaging; <http://www.fil.ion.ucl.ac.uk/spm/>). Data preprocessing in the native space included temporal and spatial alignment (i.e., slice time correction, realignment, and unwarping). Images were then spatially normalized into a standard stereotactic space (Montreal Neurological Institute), resampled to an isotropic voxel size of 2 mm × 2 mm × 2 mm, and spatially smoothed with a Gaussian kernel of 8 mm full width at half maximum. Pre-processing did not include high pass filtering or global mean correction. Model specification on single subject level included the experimental condition “response inhibition” and “reward” with *response inhibition* being related to target processing and reward was determined in terms of “win trials – loss trials.” In addition to the experimental conditions, “error trials” and “realignment parameters” (i.e., six regressors containing movement in three spatial and three rotational axes) were specified as nuisance regressors to reduce error variance and correct for movement artifacts. Condition-specific onset times were extracted from experimental log-files with onsets of the target trials defined at the moment, the target picture appeared, and onset times of reward trials locked to the time points when the reward feedback picture appeared on the screen. The onsets of error trials were defined as the target onsets of incorrect trials.

Time Series Extraction

Exact coordinates of ROIs were defined based on the significantly activated brain regions of “response inhibition”- and “reward” processing resulting from one sample *t*-tests. The local maxima of each significantly activated regions were identified and coordinates were then used as the center of a 10 mm spheric ROI using MarsBar (Brett et al., 2002). ROIs were built and used for the extraction of the time series for each subject. Time series extraction was performed using the routine as suggested by Brett et al. (2002)¹ from preprocessed fMRI data (i.e., smoothed files resulting from the pre-processing procedure; Brett et al., 2002). Finally, linear trend removal was performed between the first and the last data point of the extracted time series [using the matlab routine `detrend (y)`] (Bai et al., 2008; Zhang et al., 2008; Fox et al., 2009; Qiu et al., 2011). Linear detrending is a necessary pre-processing step, as fMRI time series have slowly varying trends, that should be removed before performing spectral analyses (Tanabe et al., 2002).

2.5 adaptive fractal analysis- AFAMultiple investigations showed that long memory is an attribute, a property of functional

networks and H is the mathematical expression, used to quantify it. Long memory processes belong to a wider range of processes, all expressing a power law spectrum (Eke et al., 2000). Their power spectral density function

$$S_x(-)S_x(f) \approx C|f|^{-\beta} \quad \text{where } -1 < \beta < 3 \quad (1)$$

[β^{ACC} : $M = 0.86 \pm 0.24$, $T(103,1) = 91.01$, $p = 0.000$; β^{NACC} : $M = 0.81 \pm 0.26$, $T(103,1) = 85.04$, $p = 0.000$] and with the approximation improving as f approaches zero. Whereas fMRI signals reflect information stemming from different cognitive and physiological processes [e.g., respiratory-frequency: 0.1–0.5 Hz; cardiac-frequency range: 0.6–1.2 Hz (Cordes et al., 2001); cognition-related low-frequency band: 0.045–0.087 Hz (Yang et al., 2018)], neural activity as providing the basis of functional connectivity in particular (Biswal et al., 1995) is carried in the low frequency components of the fMRI signals (<0.1 Hz; Achard et al., 2006; Ginestet and Simmons, 2011). Such processes describe scale-free, or scale-invariant time dynamics such as temporal brain activities. Scale invariance is associated with long range correlation in time. This is the condition to check for first, to assume scale invariance. To compute the β exponent, however, different definitions and methods might be used. For β values interpretation (Eke et al., 2002) as well as the class of processes related to them see Akhrif et al. (2018).

In this study, AFA was chosen for the determination of H , a factor that reflects in a power law manner the relationship, that is intrinsic to fractal processes, between the variance of fluctuation computed around, in our case, a second order polynomial trend $v(i)$ fitted to time series within each segment w , and its size:

$$F(w) = \left[\frac{1}{N} \sum_{i=1}^N (u(i) - v(i))^2 \right]^{1/2} \sim w^H \quad (2)$$

N : length of the time series
 $w = 2n + 1$, $n = 5, 6, \dots, 13$

H was defined as the slope of the log-log diffusion plot $\log_2(F(w))$ as a function of $\log_2(w)$ (for further details see Akhrif et al., 2018).

According to the dichotomous fGn/fBm model of Mandelbrot and Van Ness (1968) as introduced in the fractal time series analysis field by Eke et al. (2000, 2002), signal classification was performed (Mandelbrot and Van Ness, 1968; Eke et al., 2000, 2002). One of three methods of signal classification was detrended fluctuation analysis (DFA) of Peng et al. (1994). Since AFA results (H), with AFA being strongly related to DFA, were significantly smaller than 1 in both regions [H^{ACC} : $M = 0.93 \pm 0.12$, $T(103,1) = 5.95$, $p = 0.000$; H^{NACC} : $M = 0.91 \pm 0.13$, $T(103,1) = 7.22$, $p = 0.000$], signals were classified fGn, and $H = H_{fGn}$.

Brain Activation

On single subject level, two contrasts of interest were calculated, “response inhibition” to isolate target-induced brain activation, and “reward” in terms of “win-loss” to identify brain activation associated with the receipt of monetary reward. All brain analyses were performed in a region of interest (ROI) based approach,

¹<http://marsbar.sourceforge.net/marsbar.pdf>

using atlases within the Wake Forest University PickAtlas toolbox,² and covering the WI network regions: bilateral superior frontal gyrus, MFG, orbital, triangular, and opercular parts of inferior frontal gyrus (IFG), ACC, HC, and AMY, NAcc, and medial fronto-orbital gyrus. Resulting contrast images entered statistical group analysis.

Neural Network Connectivity (DCM)

For DCM analysis, DCM 12 was used as implemented in the SPM12 software. The current network included eight regions, resulting from significantly activated WI network regions (see **Table 1**). Endogenous connectivity and the condition-specific (i.e., response inhibition, reward) modulation of connectivity (modulatory inputs) were addressed. Subject-specific coordinates of the global maxima of activated clusters from brain activation results were used as centers for ROIs. Volume of interest spheres with a radius of 5 mm were built around the averaged coordinates in the NAcc and the AMY, and with a radius of 8 mm in all cortical regions. Different sphere sizes were chosen due to the regional volume size of the structures. Regional time series were extracted for all network regions.

Based on introduced findings, ten model families were constructed with 4 families varying connectivity within response inhibition-related network, 4 reward-associated families and 4 families across both conditions. Across all families and models, endogenous connectivity was specified for all connections, conditions-specific modulation, however, was varied as follows.

Inhibition-related families were families one to four. In family one (HC bottom-up), it was assumed that the HC influences top-down regions such as right and left MFG (family 1, model 1), the ACC (family 1, model 2), and both, MFG and ACC (family 1, model 3). Families two to four varied top-down connections bilateral from the MFG on the HC (family 2), from the ACC on HC (family 3), and MFG and ACC on the HC (family 4).

Families five to eight defined the interplay between the NAcc, AMY, and the vmPFC. Therefore, family five determined the

bottom-up signaling of the NAcc to the AMY (family 5, model 1), to the vmPFC (family 5, model 2), and both, the AMY and vmPFC (family 5, model 3). In analogy, in family 6 the AMY was defined as bottom-up structure and models varied between the targeted region NAcc (family 6, model 1), vmPFC (family 6, model 2), and both, NAcc and vmPFC (family 6, model 3). In family 7, both, NAcc and AMY were defined as bottom-up structure signaling to the vmPFC (family 7, model 1). In family eight, reward-associated top-down was defined on the NAcc (family 8, model 1), on the AMY (family 8, model 2), and on both, NAcc and AMY (family 8, model 3).

Across conditions, connections between reward-associated structures NAcc and AMY and inhibition-related MFG and ACC were defined in terms of family 9: NAcc – bottom-up signaling to the MFG (family 9, model 1), the MFG and the ACC (family 9, model 2), the MFG and the HC (family 9, model 3) as well as the MFG, the HC and the ACC (family 9, model 4). Family 10 defined HC and NAcc combined bottom-up signaling. Families 11 to 13 varied MFG and ACC top-down modulation of NAcc and AMY (for all models see **Supplementary Table S1**).

The families covering 28 models were compared applying random-effects Bayesian model selection (Stephan and Friston, 2010; Stephan et al., 2010) within a pre-specified Occam's window ($p < 0.05$). Individual parameter estimates of the model with highest evidence were then assessed by means of random-effects Bayesian model averaging (Penny et al., 2010) across the models of the winning family. The Bayesian model averaging parameter estimates were then entered into summary statistics at the group level. The significance of each parameter was assessed by a one-sample t -test. To test condition-specific modulation of connectivity for significance, repeated measure ANOVA models were defined with the within-subject factor *connectivity type* (endogenous connectivity vs. condition-specific modulatory input). Threshold for statistical significance was $p < 0.05$, FDR-corrected for multiple comparisons (Benjamini and Hochberg, 1995).

²<http://fmri.wfubmc.edu/software/pickatlas>

TABLE 1 | Global maxima of WI-associated brain regions.

Condition	Brain region			Z	Localization
	x	y	z		
Response inhibition	24	-28	-6	21.3	Right HC
	-22	-28	-6	17.7	Left HC
	-44	6	28	21.7	Left MFG
	40	8	34	19.7	Right MFG
	6	30	28	18.6	Right ACC
	8	12	-10	14.6	NAcc
Reward	-10	8	-14	14.7	NAcc
	-22	0	-12	5.5	Left amygdala
	0	48	-12	6.5	vmPFC

ACC, anterior cingulate cortex; HC, hippocampus; MFG, middle frontal gyrus; NAcc, nucleus accumbens; vmPFC, ventro-medial prefrontal cortex, $p < 0.05$, and FWE-corrected on voxel-level.

Statistical Analysis: Brain Activation and AFA

To address the relation between H_{fGn} deviation and network function, $1 - H_{fGn}$ scores were calculated. On group level, two sample t -tests were defined with the group factor impulsive phenotype (highIMP vs. lowIMP) including the covariates H_{fGn}^{ACC} and H_{fGn}^{NAcc} alterations and determined as interacting with the group factor. Contrast of interest were (i) the correlation between alterations in H_{fGn} and brain activation across all subjects (e.g., response inhibition * H_{fGn}^{ACC} alterations) as well as (ii) group-specific correlations (e.g., response inhibition * H_{fGn}^{ACC} alterations: highIMP vs. lowIMP). The between-subject factor *impulsivity* classified subjects based on behavioral performance [i.e., a number of premature responses ≥ 3 in the 5-CSRTT as highIMP ($n = 38$) subjects and subjects with number of premature responses < 3 as lowIMP ($n = 65$) subjects]. Threshold of significance was $p_{FWE} < 0.05$ on voxel level.

RESULTS

fMRI Analysis

One sample *t*-tests of *response inhibition* and *reward* revealed a significantly activated WI network including the regions right/left HC, right/left MFG, ACC, right/left NAcc, left AMY, and the vmPFC (Table 1).

Dynamic Causal Modeling Estimates

Model comparison favored the reward-related NAcc + Amy bottom-up model 1 of family 7, with a family exceedance probability of $x_p = 0.8353$ and a model exceedance probability of $x_p = 0.9954$. In the winning model, endogenous connectivity included all connections, and reward-related modulatory input bidirectional connectivity between the NAcc and the AMY and going to the vmPFC (i.e., NAcc→l_AMY, NAcc→vmPFC, l_AMY→NAcc, and l_AMY→vmPFC). The one-sample *t*-test, identifying connections of significant connectivity strength revealed that almost all connections were passed the threshold of significance except for connectivity from the rHC→l_AMY ($T = 1.3, p = 0.182, n. s.$), lMFG→rHC ($T = 1.1, p = 0.275, n. s.$), r_MFG→vmPFC ($T = 0.8, p = 0.458, n.s.$), ACC→r_HC ($T = 1.1, p = 0.267, n.s.$), and vmPFC→r_MFG ($T = 0.6, p = 0.582, n.s.$). Repeated-measures ANOVA revealed significant modulation for all four connections (NAcc→l_AMY: $F_{connectivity\ type} = 37.5,$

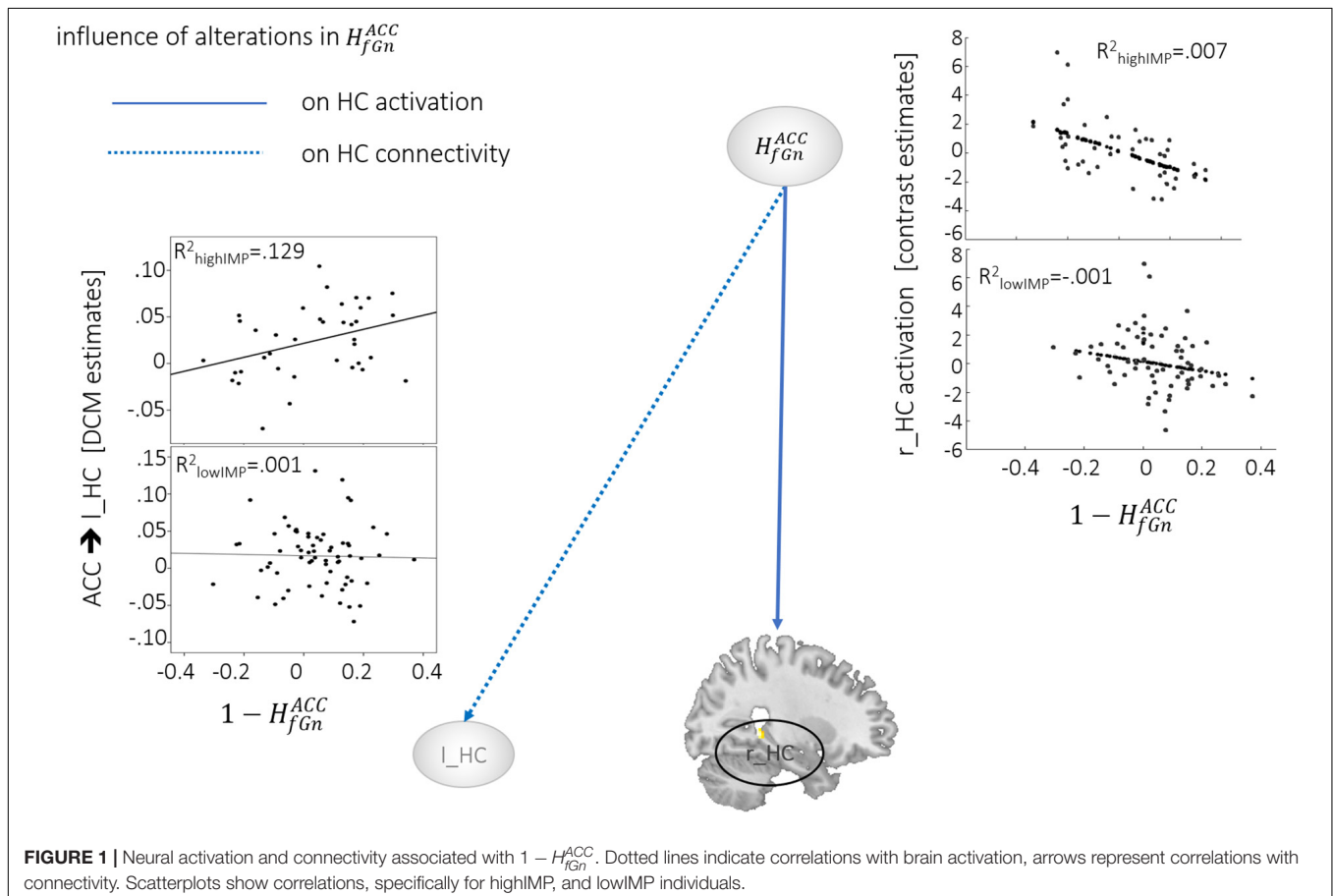
$p = 0.000$; NAcc→vmPFC: $F_{connectivity\ type} = 114.7, p = 0.000$; l_AMY→NAcc: $F_{connectivity\ type} = 40.5, p = 0.000$; and l_AMY→vmPFC: $F_{connectivity\ type} = 72.6, p = 0.000$).

Alterations in H_{fGn}^{ACC} and Network Function

During *response inhibition* brain activation in the r_HC negatively correlated with alterations in H_{fGn}^{ACC} across all subjects. The effect, however, seemed to be driven by highIMP subjects as demonstrated in the scatterplot in Figure 1. In addition, highIMP-specific positive correlations between connectivity emerging from the ACC and heading toward the l_HC (ACC→l_HC) and alterations in H_{fGn}^{ACC} were revealed. Furthermore, in lowIMP subjects H_{fGn}^{ACC} alterations correlated negatively with left-hemispheric fronto-hippocampal connectivity, i.e., l_HC bottom-up signaling to the l_MFG and frontal top-down control of the l_HC by the l_MFG (l_HC→l_MFG, l_MFG→l_HC; for all results see Tables 2, 3 and Figure 1).

Alterations in H_{fGn}^{NAcc} and Network Function

Reward-specific activation bilaterally in the dlPFC (MFG and IFG pars triangularis) correlated positively with H_{fGn}^{NAcc} alterations.



This correlation was stronger in highIMP compared to lowIMP (see **Tables 2, 3** and **Figure 2**). In addition, alterations in H_{fGn}^{NACC} correlated in highIMP but not in lowIMP subjects, with top-down control of the r_HC by the l_MFG (l_MFG→r_HC).

DISCUSSION

In this study, we investigated the relation between impulsivity-associated deviations of H_{fGn} in the ACC and the NAcc and the function of the underlying network. In an earlier publication, H_{fGn} in both regions have been found to be reduced in highIMP subjects. Current analyses revealed that deviations in the H_{fGn}^{ACC} were predominantly associated with response inhibition processing, namely right hippocampal brain activation and, specifically in highIMP subjects, connectivity from the ACC on the left HC. Likewise, deviations in H_{fGn}^{NACC} were associated with broad reward-associated activation clusters in the dlPFC as well as connectivity from the left MFG on the right HC. Findings in reward processing were only significant in highIMP subjects. Thus, across all analyses, H_{fGn} alterations seemed to be related to HC functioning, hinting toward a H_{fGn} -specific relation to HC processing.

In the WI network as proposed by Dalley et al. (2011) the HC has been assumed to directly interact with the ACC in terms of both structures top-down controlling the NAcc. Empirical evidence in humans, however, is scarce (Morris et al., 2016; Neufang et al., 2016; Mechelmans et al., 2017). Recent studies showed, that impulsivity was strongly linked to a hypothalamo-hippocampal pathway including the HC (Gruber and McDonald, 2012), and the NAcc (Barlow et al., 2018; Noble et al., 2019) with a maladaptation of HC-NAcc pathway contributing to the development of impulsivity and impulsivity-associated psychiatric disorders such as addiction (Everitt and Robbins, 2005). For example, in mice WI behavior potentiated hippocampal neurogenesis the way that during reward seeking behavior in the 5-CSRTT, precursor cells were produced in the dentate gyrus of the HC (Oliveros et al., 2017; Peyton et al., 2019). Such impulsivity-induced neurogenesis has been discussed as reflecting both reward-driven highIMP responding and (the known HC-associated) heightened learning performance (Peyton et al., 2019). Thus, it seemed, as if HC function plays a crucial role within the impulsivity network. Combining both assumptions, (i) the

TABLE 3 | Significant correlations between alterations of H_{fGn} and network connectivity.

	Connection	R_{lowIMP}	$R_{highIMP}$	Z
$1 - H_{fGn}^{ACC}$	L_HC→l_MFG	-0.32*, $p = 0.01$	0.23, $p = 0.17$	2.6*, $p = 0.01$
	l_MFG→L_HC	-0.30*, $p = 0.02$	0.21, $p = 0.21$	2.4*, $p = 0.01$
	ACC→L_HC	-0.03, $p = 0.84$	0.36*, $p = 0.03$	1.9*, $p = 0.03$
$1 - H_{fGn}^{NACC}$	l_MFG→r_HC	-0.09, $p = 0.49$	0.35*, $p = 0.03$	2.1*, $p = 0.02$

l_HC, left hippocampus; *r_HC*, right hippocampus; *l_MFG*, left middle frontal gyrus; *ACC*, anterior cingulate cortex; * $p < 0.05$; FDR-corrected for 64 comparisons (8 network regions, 8×8 connectivity matrix).

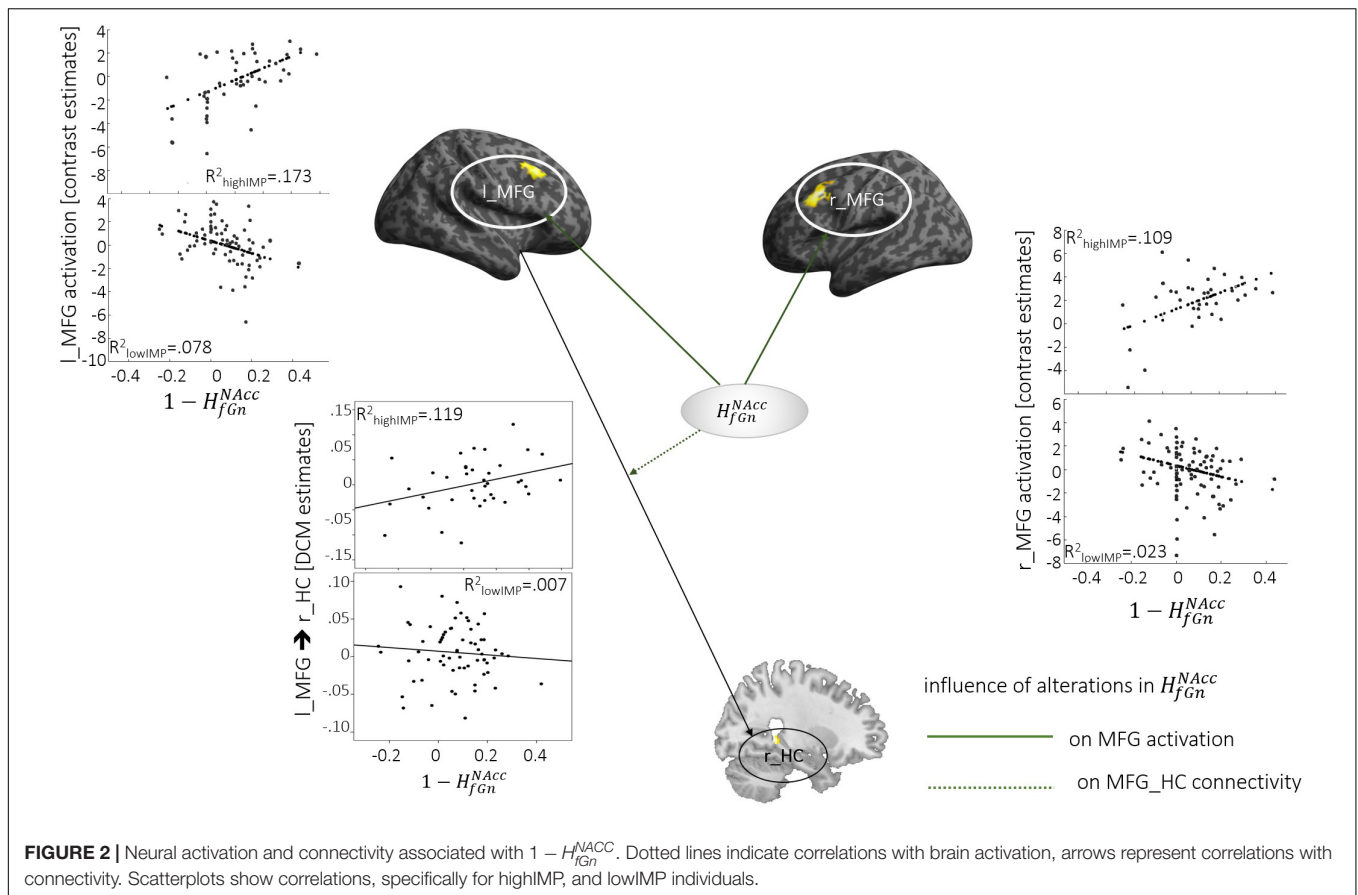
HC plays a crucial role within the network and (ii) fractal parameter such as H disentangling functional components from artifactual ones, the current strong relation between H_{fGn} and HC processing seemed plausible. An alternative explanation might be their common involvement in long-term memory. H has been used to describe long-term memory processes before, e.g., in capital markets (Di Matteo et al., 2005; Granero et al., 2008), energy future prices (Serletis and Rosenberg, 2007), and human (motor) memory (Chen et al., 1997; Namazi, 2018). The 5-CSRTT, in return, involves a high learning and memory load as the training and test protocol for animals covers numerous training sessions over weeks (“approximately 30–40 daily sessions,” Bari et al., 2008). Thus, in our analyses, the H_{fGn} exponent proved its strong relation to learning and memory processing even when further prominent cognitive functions such as reward processing were involved.

In addition to HC, altered H_{fGn} was associated with frontal activation and connectivity. The MFG and the IFG are core regions within impulsivity and WI (Dalley et al., 2011), strongly interacting with the ACC (Mechelmans et al., 2017), and implicated in response inhibition and motor control (Morris et al., 2016; Neufang et al., 2016; Mechelmans et al., 2017). Association between H and the frontal cortex have been reported in numerous human studies before. For example, H in the prefrontal cortex in healthy volunteers correlated with impulsivity (Gentili et al., 2020), personality traits (e.g., extraversion Lei et al., 2013; Gentili et al., 2017), cognitive processing (response time in a face recognition task Wink et al., 2008), and healthy aging (Dong et al., 2018; Mukli et al., 2018). In addition, pathological processes were discovered, e.g., in the IFG of schizophrenic

TABLE 2 | Significant correlations between alterations in H_{fGn} and brain activation.

Condition	Contrast	Brain region			Z	Localization
		x	y	z		
Response inhibition * $1 - H_{fGn}^{ACC}$	(lowIMP + highIMP) ⁽⁻⁾	26	-42	0	4.1, $p = 0.054$	Right HC
Reward * $1 - H_{fGn}^{NACC}$	highIMP > lowIMP	-42	12	42	4.8, $p = 0.004$	Left MFG
		40	20	44	4.6, $p = 0.006$	Right MFG
		50	34	-2	4.4, $p = 0.018$	Right IFG
		-44	18	8	4.3, $p = 0.022$	Left IFG

⁽⁻⁾, negative correlation; HC, hippocampus; MFG, middle frontal gyrus; IFG, inferior frontal gyrus; p , triangularis, $p < 0.05$, and FWE-corrected on voxel-level.



patients (Sokunbi et al., 2014), the MFG of patients with mild cognitive impairment (Long et al., 2016, 2018), and Alzheimer's Disease (Nimmy John et al., 2018) as well as the IFG of autistic individuals (Lai et al., 2010). Thus, frontal processing has been described as following fractal rules before. In line with our findings, H seemed to be able to detect neural alterations not only in pathological populations but also in individual variability in the normal population (Serletis et al., 2012).

In summary, in this study, we addressed the relation between altered H_{fGn} and further neural network parameters in an explorative way to get an idea of how deviations in H_{fGn} were associated with neural network functioning. We found that alterations in H_{fGn} were predominantly related in fronto-hippocampal pathways arguing, that H_{fGn} proved its sensitivity toward learning and memory processing. However, despite the highly interesting and plausible results, we have to state, the current findings reflect processes within a very specific sample (young healthy male students) performing the also very specialized 5-CSRTT (a paradigm which has, to date, predominantly been used in animals). In addition, in contrast to earlier publications, where the interaction between several physiological systems such as brain and cardiac system (Liu et al., 2015, Lin et al., 2016), or brain, cardiac and respiratory systems (Bartsch and Ivanov, 2014) were addressed over phases of different physiological states, analysis of the current work

was limited to one physiological network and only during one single state. Especially the frontal lobe seemed to interact with the heart as has been shown in several studies by Thayer et al. (2009, 2012) and Patron et al. (2019). In addition, this data stems from a sample of male subjects only. The data has been collected in a pilot study, which has been published 2016 as the first fMRI study using the human version of the originally animal paradigm 5-CSRTT (Neufang et al., 2016). As at that time, network regions associated with WI in humans was mainly theoretical, we decided to investigate neural underpinnings in a highly homogenous sample, which is healthy male students. Thus, findings are of limited generalizability and need to be replicated in future studies with experimental protocols like those published before. However, the combination of H with further cognitive, neural and peripheral parameters such as inflammation scores as well as the longitudinal study of H to describe physiological variations (e.g., diurnal, brain maturation, aging) are of highest interest in the study of neural networks.

DATA AVAILABILITY STATEMENT

The datasets generated for this study are available on request to the corresponding author.

ETHICS STATEMENT

The studies involving human participants were reviewed and approved by Ethics Committee of the Faculty of Medicine, University of Würzburg. The patients/participants provided their written informed consent to participate in this study.

AUTHOR CONTRIBUTIONS

AA was responsible for H data analysis. SN performed brain activation and connectivity analyses. All authors equally contributed to manuscript writing.

REFERENCES

- Abry, P., Goncalves, P., and V  hel, J. L. (2013). *Scaling, Fractals and Wavelets*. Hoboken, NJ: John Wiley & Sons.
- Achard, S., Salvador, R., Whitcher, B., Suckling, J., and Bullmore, E. (2006). A resilient, low-frequency, small-world human brain functional network with highly connected association cortical hubs. *J. Neurosci.* 26, 63–72. doi: 10.1523/jneurosci.3874-05.2006
- Akhrif, A., Romanos, M., Domschke, K., Schmitt-Boehrer, A., and Neufang, S. (2018). Fractal analysis of BOLD time series in a network associated with waiting impulsivity. *Front. Physiol.* 9:1378. doi: 10.3389/fphys.2018.01378
- Bai, F., Zhang, Z., Yu, H., Shi, Y., Yuan, Y., Zhu, W., et al. (2008). Default-mode network activity distinguishes amnesic type mild cognitive impairment from healthy aging: a combined structural and resting-state functional MRI study. *Neurosci. Lett.* 438, 111–115. doi: 10.1016/j.neulet.2008.04.021
- Bari, A., Dalley, J. W., and Robbins, T. W. (2008). The application of the 5-choice serial reaction time task for the assessment of visual attentional processes and impulse control in rats. *Nat. Protoc.* 3, 759–767. doi: 10.1038/nprot.2008.41
- Barlow, R. L., Gorges, M., Wearn, A., Niessen, H. G., Kassubek, J., Dalley, J. W., et al. (2018). Ventral Striatal D2/3 Receptor availability is associated with impulsive choice behavior as well as limbic corticostriatal connectivity. *Int. J. Neuropsychopharmacol.* 21, 705–715. doi: 10.1093/ijnp/pyy030
- Bartsch, R. P., and Ivanov, P. C. (2014). “Coexisting forms of coupling and phase-transitions in physiological networks,” in *International Conference on Nonlinear Dynamics of Electronic Systems*, Berlin: Springer, 270–287. doi: 10.1007/978-3-319-08672-9_33
- Benjamini, Y., and Hochberg, Y. (1995). Controlling the false discovery rate: a practical and powerful approach to multiple testing. *J. R. Stat. Soc. Ser. B* 57, 289–300. doi: 10.1111/j.2517-6161.1995.tb02031.x
- Biswal, B., Zerrin Yetkin, F., Haughton, V. M., and Hyde, J. S. (1995). Functional connectivity in the motor cortex of resting human brain using echo-planar MRI. *Magnet. Reson. Med.* 34, 537–541. doi: 10.1002/mrm.1910340409
- Brett, M., Anton, J.-L., Valabregue, R., and Poline, J.-P. (2002). “Region of interest analysis using an SPM toolbox [abstract],” in *Neuroimage International Conference on Functional Mapping of the Human Brain*, Sendai, 497.
- Chen, Y., Ding, M., and Kelso, J. S. (1997). Long memory processes (1/f α type) in human coordination. *Phys. Rev. Lett.* 79:4501. doi: 10.1103/physrevlett.79.4501
- Ciuciu, P., Varoquaux, G., Abry, P., Sadaghiani, S., and Kleinschmidt, A. (2012). Scale-free and multifractal time dynamics of fMRI signals during rest and task. *Front. Physiol.* 3:186. doi: 10.3389/fphys.2012.00186
- Cordes, D., Haughton, V. M., Arfanakis, K., Carew, J. D., Turski, P. A., Moritz, C. H., et al. (2001). Frequencies contributing to functional connectivity in the cerebral cortex in “resting-state” data. *AJNR Am. J. Neuroradiol.* 22, 1326–1333.
- Dalley, J. W., Everitt, B. J., and Robbins, T. W. (2011). Impulsivity, compulsivity, and top-down cognitive control. *Neuron* 69, 680–694. doi: 10.1016/j.neuron.2011.01.020
- Di Matteo, T., Aste, T., and Dacorogna, M. M. (2005). Long-term memories of developed and emerging markets: using the scaling analysis to characterize their stage of development. *J. Bank. Finance* 29, 827–851. doi: 10.1016/j.jbankfin.2004.08.004
- Dona, O., Hall, G. B., and Noseworthy, M. D. (2017a). Temporal spectral analysis of the rs-BOLD signal identifies brain abnormalities in autism spectrum disorder. *PLoS One* 12:e0190081. doi: 10.1371/journal.pone.0190081
- Dona, O., Noseworthy, M. D., Dematteo, C., and Connolly, J. F. (2017b). Fractal analysis of brain blood oxygenation level dependent (BOLD) signals from children with mild traumatic brain injury (mTBI). *PLoS One* 12:e0169647. doi: 10.1371/journal.pone.0169647
- Dong, J., Jing, B., Ma, X., Liu, H., Mo, X., and Li, H. (2018). Hurst exponent analysis of resting-State fMRI signal complexity across the adult lifespan. *Front. Neurosci.* 12:34. doi: 10.3389/fnins.2018.00034
- Eke, A., Herman, P., Bassingthwaite, J. B., Raymond, G. M., Percival, D. B., Cannon, M., et al. (2000). Physiological time series: distinguishing fractal noises from motions. *Pflugers Arch.* 439, 403–415. doi: 10.1007/s004240050957
- Eke, A., Herman, P., Kocsis, L., and Kozak, L. R. (2002). Fractal characterization of complexity in temporal physiological signals. *Physiol. Meas.* 23, R1–R38.
- Everitt, B. J., and Robbins, T. W. (2005). Neural systems of reinforcement for drug addiction: from actions to habits to compulsion. *Nat. Neurosci.* 8, 1481–1489. doi: 10.1038/nn1579
- Fox, M. D., Zhang, D., Snyder, A. Z., and Raichle, M. E. (2009). The global signal and observed anticorrelated resting state brain networks. *J. Neurophysiol.* 101, 3270–3283. doi: 10.1152/jn.90777.2008
- Gentili, C., Cristea, I. A., Ricciardi, E., Vanello, N., Popita, C., David, D., et al. (2017). Not in one metric: neuroticism modulates different resting state metrics within distinctive brain regions. *Behav. Brain Res.* 327, 34–43. doi: 10.1016/j.bbr.2017.03.031
- Gentili, C., Vanello, N., Podina, I., Popita, R., Voinescu, B., Pietrini, P., et al. (2020). You do not have to act to be impulsive: brain resting-state activity predicts performance and impulsivity on the balloon analogue risk task. *Behav. Brain Res.* 379:112395. doi: 10.1016/j.bbr.2019.112395
- Ginestet, C. E., and Simmons, A. (2011). Statistical parametric network analysis of functional connectivity dynamics during a working memory task. *Neuroimage* 55, 688–704. doi: 10.1016/j.neuroimage.2010.11.030
- Goldberger, A. L., Amaral, L. A., Hausdorff, J. M., Ivanov, P., Peng, C. K., and Stanley, H. E. (2002). Fractal dynamics in physiology: alterations with disease and aging. *Proc. Natl. Acad. Sci. U.S.A.* 99(Suppl. 1), 2466–2472. doi: 10.1073/pnas.012579499
- Granero, M. S., Segovia, J. T., and P  rez, J. G. (2008). Some comments on Hurst exponent and the long memory processes on capital markets. *Phys. A Stat. Mech. Appl.* 387, 5543–5551. doi: 10.1016/j.physa.2008.05.053
- Gruber, A. J., and McDonald, R. J. (2012). Context, emotion, and the strategic pursuit of goals: interactions among multiple brain systems controlling motivated behavior. *Front. Behav. Neurosci.* 6:50. doi: 10.3389/fnbeh.2012.00050
- Lai, M. C., Lombardo, M. V., Chakrabarti, B., Sadek, S. A., Pasco, G., Wheelwright, S. J., et al. (2010). A shift to randomness of brain oscillations in people with autism. *Biol. Psychiatry* 68, 1092–1099. doi: 10.1016/j.biopsych.2010.06.027

FUNDING

SN were funded by the Deutsche Forschungsgemeinschaft (DFG, German Research Foundation) – Project Number 44541416 – TRR 58 and – Project Number 404502177.

SUPPLEMENTARY MATERIAL

The Supplementary Material for this article can be found online at: <https://www.frontiersin.org/articles/10.3389/fphys.2020.00827/full#supplementary-material>

FIGURE S1 | A representative experimental trial.

TABLE S1 | DCM families and models.

- Lei, X., Zhao, Z., and Chen, H. (2013). Extraversion is encoded by scale-free dynamics of default mode network. *Neuroimage* 74, 52–57. doi: 10.1016/j.neuroimage.2013.02.020
- Lin, A., Liu, K. K., Bartsch, R. P., and Ivanov, P. C. (2016). Delay-correlation landscape reveals characteristic time delays of brain rhythms and heart interactions. *Philos. Trans. R. Soc. A Math. Phys. Eng. Sci.* 374:20150182. doi: 10.1098/rsta.2015.0182
- Lipsitz, L. A., and Goldberger, A. L. (1992). Loss of complexity and aging: potential applications of fractals and chaos theory to senescence. *JAMA* 267, 1806–1809. doi: 10.1001/jama.267.13.1806
- Liu, K. K., Bartsch, R. P., Lin, A., Mantegna, R. N., and Ivanov, P. C. (2015). Plasticity of brain wave network interactions and evolution across physiologic states. *Front. Neural Circ.* 9:62. doi: 10.3389/fncir.2015.00062
- Long, Z., Jing, B., Guo, R., Li, B., Cui, F., Wang, T., et al. (2018). A brainnetome atlas based mild cognitive impairment identification using hurst exponent. *Front. Aging Neurosci.* 10:103. doi: 10.3389/fnagi.2018.00103
- Long, Z., Jing, B., Yan, H., Dong, J., Liu, H., Mo, X., et al. (2016). A support vector machine-based method to identify mild cognitive impairment with multi-level characteristics of magnetic resonance imaging. *Neuroscience* 331, 169–176. doi: 10.1016/j.neuroscience.2016.06.025
- Mandelbrot, B. B., and Van Ness, J. W. (1968). Fractional brownian motions, fractional noises and applications. *SIAM Rev.* 10, 422–437. doi: 10.1137/1010093
- Mechelmans, D. J., Strelchuk, D., Donamayor-Alonso, N., Banca, P., Robbins, T. W., Baek, K., et al. (2017). Reward sensitivity and waiting impulsivity: shift towards reward valuation away from action control. *Int. J. Neuropsychopharmacol.* 20, 971–978. doi: 10.1093/ijnp/pyx072
- Morris, L. S., Kundu, P., Baek, K., Irvine, M. A., Mechelmans, D. J., Wood, J., et al. (2016). Jumping the gun: mapping neural correlates of waiting impulsivity and relevance across alcohol misuse. *Biol. Psychiatry* 79, 499–507. doi: 10.1016/j.biopsych.2015.06.009
- Mukli, P., Nagy, Z., Racz, F. S., Herman, P., and Eke, A. (2018). Impact of healthy aging on multifractal hemodynamic fluctuations in the human prefrontal cortex. *Front. Physiol.* 9:1072. doi: 10.3389/fphys.2018.01072
- Namazi, H. (2018). Can we mathematically correlate brain memory and complexity. *ARC J.* 216, 1–3.
- Neufang, S., Akhrif, A., Herrmann, C. G., Drepper, C., Homola, G. A., Nowak, J., et al. (2016). Serotonergic modulation of 'waiting impulsivity' is mediated by the impulsivity phenotype in humans. *Transl. Psychiatry* 6:e940. doi: 10.1038/tp.2016.210
- Nimmy John, T., Puthankattil, S. D., and Menon, R. (2018). Analysis of long range dependence in the EEG signals of Alzheimer patients. *Cogn. Neurodyn.* 12, 183–199. doi: 10.1007/s11571-017-9467-8
- Noble, E. E., Wang, Z., Liu, C. M., Davis, E. A., Suarez, A. N., Stein, L. M., et al. (2019). Hypothalamus-hippocampus circuitry regulates impulsivity via melanin-concentrating hormone. *Nat. Commun.* 10:4923.
- Oliveros, A., Cho, C. H., Cui, A., Choi, S., Lindberg, D., Hinton, D., et al. (2017). Adenosine A2A receptor and ERK-driven impulsivity potentiates hippocampal neuroblast proliferation. *Transl. Psychiatry* 7:e1095. doi: 10.1038/tp.2017.64
- Patron, E., Mennella, R., Messerotti Benvenuti, S., and Thayer, J. F. (2019). The frontal cortex is a heart-brake: reduction in delta oscillations is associated with heart rate deceleration. *Neuroimage* 188, 403–410. doi: 10.1016/j.neuroimage.2018.12.035
- Peng, C.-K., Buldyrev, S. V., Havlin, S., Simons, M., Stanley, H. E., and Goldberger, A. L. (1994). Mosaic organization of DNA nucleotides. *Phys. Rev.* 49:1685. doi: 10.1103/physreve.49.1685
- Penny, W. D., Stephan, K. E., Daunizeau, J., Rosa, M. J., Friston, K. J., Schofield, T. M., et al. (2010). Comparing families of dynamic causal models. *PLoS Comput. Biol.* 6:e1000709. doi: 10.1371/journal.pcbi.1000709
- Peyton, L., Oliveros, A., Cho, C. H., Starski, P., Lindberg, D., Jang, M. H., et al. (2019). Waiting impulsivity during reward seeking increases adult hippocampal neurogenesis in mice. *Neurosci. Lett.* 706, 169–175. doi: 10.1016/j.neulet.2019.05.032
- Pipiras, V., and Taqqu, M. S. (2017). *Long-Range Dependence and Self-Similarity*. Cambridge: Cambridge University Press.
- Qiu, Y. W., Han, L. J., Lv, X. F., Jiang, G. H., Tian, J. Z., Zhuo, F. Z., et al. (2011). Regional homogeneity changes in heroin-dependent individuals: resting-state functional MR imaging study. *Radiology* 261, 551–559. doi: 10.1148/radiol.11102466
- Rösler, M., Retz, W., Retz-Junginger, P., Stieglitz, R., Kessler, H., Reimherr, F., et al. (2008). ADHS-diagnose bei erwachsenen. *Der. Nervenarzt.* 79, 320–327.
- Serletis, A., and Rosenberg, A. A. (2007). The Hurst exponent in energy futures prices. *Phys. A Stat. Mech. Appl.* 380, 325–332. doi: 10.1016/j.physa.2007.02.055
- Serletis, D., Bardakjian, B. L., Valiante, T. A., and Carlen, P. L. (2012). Complexity and multifractality of neuronal noise in mouse and human hippocampal epileptiform dynamics. *J. Neural Eng.* 9:056008. doi: 10.1088/1741-2560/9/5/056008
- Sokunbi, M. O., Gradin, V. B., Waiter, G. D., Cameron, G. G., Ahearn, T. S., Murray, A. D., et al. (2014). Nonlinear complexity analysis of brain fMRI signals in schizophrenia. *PLoS One* 9:e95146. doi: 10.1371/journal.pone.0095146
- Stephan, K. E., and Friston, K. J. (2010). Analyzing effective connectivity with functional magnetic resonance imaging. *Wiley Interdiscip. Rev. Cogn. Sci.* 1, 446–459. doi: 10.1002/wcs.58
- Stephan, K. E., Penny, W. D., Moran, R. J., Den Ouden, H. E., Daunizeau, J., and Friston, K. J. (2010). Ten simple rules for dynamic causal modeling. *Neuroimage* 49, 3099–3109. doi: 10.1016/j.neuroimage.2009.11.015
- Tanabe, J., Miller, D., Tregellas, J., Freedman, R., and Meyer, F. G. (2002). Comparison of detrending methods for optimal fMRI preprocessing. *NeuroImage* 15, 902–907. doi: 10.1006/nimg.2002.1053
- Taylor, P. A., Gohel, S., Di, X., Walter, M., and Biswal, B. B. (2012). Functional covariance networks: obtaining resting-state networks from intersubject variability. *Brain Connect* 2, 203–217. doi: 10.1089/brain.2012.0095
- Thayer, J. F., Ahs, F., Fredrikson, M., Sollers, J. J. III, and Wager, T. D. (2012). A meta-analysis of heart rate variability and neuroimaging studies: implications for heart rate variability as a marker of stress and health. *Neurosci. Biobehav. Rev.* 36, 747–756. doi: 10.1016/j.neubiorev.2011.11.009
- Thayer, J. F., Hansen, A. L., Saus-Rose, E., and Johnsen, B. H. (2009). Heart rate variability, prefrontal neural function, and cognitive performance: the neurovisceral integration perspective on self-regulation, adaptation, and health. *Ann. Behav. Med.* 37, 141–153. doi: 10.1007/s12160-009-9101-z
- Voon, V., Irvine, M. A., Derbyshire, K., Worbe, Y., Lange, I., Abbott, S., et al. (2014). Measuring "waiting" impulsivity in substance addictions and binge eating disorder in a novel analogue of rodent serial reaction time task. *Biol. Psychiatry* 75, 148–155. doi: 10.1016/j.biopsych.2013.05.013
- Wink, A. M., Bernard, F., Salvador, R., Bullmore, E., and Suckling, J. (2006). Age and cholinergic effects on hemodynamics and functional coherence of human hippocampus. *Neurobiol. Aging* 27, 1395–1404. doi: 10.1016/j.neurobiolaging.2005.08.011
- Wink, A. M., Bullmore, E., Barnes, A., Bernard, F., and Suckling, J. (2008). Monofractal and multifractal dynamics of low frequency endogenous brain oscillations in functional MRI. *Hum. Brain. Mapp.* 29, 791–801. doi: 10.1002/hbm.20593
- Yang, A. C., Tsai, S. J., Lin, C. P., Peng, C. K., and Huang, N. E. (2018). Frequency and amplitude modulation of resting-state fMRI signals and their functional relevance in normal aging. *Neurobiol. Aging* 70, 59–69. doi: 10.1016/j.neurobiolaging.2018.06.007
- Zhang, D., Snyder, A. Z., Fox, M. D., Sansbury, M. W., Shimony, J. S., and Raichle, M. E. (2008). Intrinsic functional relations between human cerebral cortex and thalamus. *J. Neurophysiol.* 100, 1740–1748. doi: 10.1152/jn.90463.2008

Conflict of Interest: The authors declare that the research was conducted in the absence of any commercial or financial relationships that could be construed as a potential conflict of interest.

Copyright © 2020 Neufang and Akhrif. This is an open-access article distributed under the terms of the Creative Commons Attribution License (CC BY). The use, distribution or reproduction in other forums is permitted, provided the original author(s) and the copyright owner(s) are credited and that the original publication in this journal is cited, in accordance with accepted academic practice. No use, distribution or reproduction is permitted which does not comply with these terms.